ELSEVIER

Journal of Power Sources 68 (1997) 421–426

JOURNAL OF POWER SOURCES

Formation of perovskite solid solutions and lithium-ion conductivity in the compositions, $Li_{2x}Sr_{1-2x}M^{III}_{0.5-x}Ta_{0.5+x}O_3$ (M = Cr, Fe, Co, Al, Ga, In, Y)

Hiroyuki Watanabe, Jun Kuwano *

Department of Industrial Chemistry, Faculty of Engineering, Science University of Tokyo, 1-3 Kagurazaka, Shinjuku-ku, Tokyo 162, Japan

Accepted 3 March 1997

Abstract

Formation of solid solutions with perovskite structure and ionic conductivity have been investigated in the systems $Li_{2x}Sr_{1-2x}M^{III}_{0.5-x}Ta_{0.5+x}O_3$ (M = Cr, Fe, Co, Al, Ga, In, Y). Perovskite solid solutions formed in ranges of $x \leq 0.25$ for M = Fe, Cr, $x < 0.22$ for Ga and $x < \sim 0.16$ for M = Co, In. No single-phase samples of perovskite solid solution were prepared for M = Al, Y. The solid solutions $Li_{0.5}Sr_{0.5}M^{III}_{0.25}Ta_{0.75}O_3$ (M = Fe, Cr; $x = 0.25$) had high bulk conductivities of 1.0×10^{-4} S cm^{-1} and 6.0×10^{-5} S cm^{-1} at room temperature, respectively. The former value was the highest of those reported to date for lithium electrolytes based on tantalates. They were simple cubic perovskites (space group: *Pm3m*; $a = 396.39$ pm for Fe, $a = 395.03$ pm for Cr), indicating that the Li and Sr ions, and the M (Fe or Cr) and Ta ions are randomly distributed over the A-sites and B-sites, respectively. Frame emission analysis for Li in both sintered pellets revealed that the loss of the Li content took place during sintering. The high conductivity is probably attributed to an A-site deficient perovskite phase resulting from the loss. The perovskite solid solutions in the other systems exhibited conductivities as low as 10^{-7}–10^{-8} S cm^{-1}. The Fe- and Cr-containing solid solutions are the first of tantalate-based perovskites with high Li-ion conductivity. © 1997 Elsevier Science S.A.

Keywords: Lithium-ion conductivity; Perovskite; Ionic conductivity; Solid electrolytes; Tantalate; Ionic conductors

1. Introduction

A wide variety of solid electrolytes with high ionic conductivity has been discovered for the last two decades [1]. Lithium-ion conductors are among the most attractive, because Li systems [2] hold the great promise of high energy density batteries, owing to reasonable cost, high open-circuit voltages and low equivalent weights. However, no Li solid-state cells have been put into practical use with a few exception of those used in cardiac pacemakers [3].

In solid electrolytes, most attention tends to be paid to the magnitude of ionic conductivity. However, the practical use is often limited by properties other than ionic conductivity. The main problem in the development of Li solid-state cells is the absence of Li solid electrolytes with both high ionic conductivity and other requisite properties, for example, chemical stability with Li metal and cathode active materials, and high decomposition potential, ease of preparation and processing, etc. Thus, of great interest is the possibility of finding suitable Li solid electrolytes that can be employed in the solid-state batteries.

It is an exciting topic that high Li-ion conductivities of $\sim 10^{-3}$–10^{-4} S cm^{-1} at room temperature have been discovered in titanate-based solid solutions with perovskite-related structures, such as $Li_{3x}Ln_{0.67-x}TiO_3$: Ln = La [4–8], (La, Nd) [7]; $Li_xSr_{1-x}Ta_xTi_{1-x}O_3$ [9]. They are one of the families with the highest conductivities so far reported for Li-ion conducting materials. A recent study [10] on the crystal structure of the $Li_{3x}Ln_{0.67-x}TiO_3$ (Ln = Pr, Nd) solid solutions have suggested that the Li-ion conduction in the perovskite-related solid solutions occurs by an ion-vacancy mechanism through the interconnecting A-sites, making a detour round those sites that are occupied by the Ln^{3+} cations. Three polymorphic forms were found in an extensive range of the $Li_{3x}La_{0.67-x}TiO_3$ solid solution: the high-temperature form with a simple cubic perovskite unit cell and the intermediate- and low-temperature forms with tetragonal, doubled perovskite unit cells [11]. Very interestingly, at a composition close to $Li_{0.5}La_{0.5}TiO_3$, the macro-domain texture con-

* Corresponding author: Tel.: +81 (3) 3260-4271, ext 3487; Fax +81 (3) 5261-4631.

PII S0378-7753(97)02645-1

sisting of different superstructural cells has been observed by high resolution transmission microscopy [12].

Tetravalent Ti ions are readily reduced to the trivalent ions. For example, the Li analogues of NASICONs [13,14] exhibited ionic conductivities of $\sim 10^{-3}$–10^{-4} S cm^{-1} at room temperature, comparable with those of the perovskite-related solid solutions. They are titanate-based compounds and suffer from the reducible nature [15]. Unfortunately, the perovskite-related solid solutions found to date also are titanate-based compounds and are unstable with Li metal [5]. The Li analogues of NASICONs and the perovskite-related solid solutions have been reported to have the capability of Li intercalation [15,16]. Thus, they can be used as the cathode-active material rather than the electrolyte in Li solid-state batteries.

The Li-ion conductivity in the perovskite-related solid solutions of the series $Li_{3x}Ln_{0.67-x}TiO_3$ depended on the perovskite subcell volume, i.e., the size of the A-sites ion (i.e., Ln ion) other than Li ion [7,17], because the perovskite framework is propped with Ln ions only. Lanthanum ions are the largest of practically available trivalent ions. Thus, it would be very attractive to synthesize perovskite-related solid solutions containing no Ti ions for improvement of the reducible nature and Li-ion conductivity, by replacement of La^{3+} and Ti^{4+} ions by larger Sr^{2+} ions and less reducible Ta^{5+} ions, respectively. Furthermore, no Li-ion conducting perovskites based on tantalates have been reported so far.

In this study, we attempt to prepare perovskite-related solid solutions with high Li-ion conductivity in the series $Li_{2x}Sr_{1-2x}M^{III}_{0.5-x}Ta_{0.5+x}O_3$ (M = Cr, Fe, Co, Al, Ga, In, Y) and examine their electrical properties.

2. Experimental

Reagent grade $Sr(NO_3)_2$, Li_2CO_3, Ta_2O_5 and M_2O_3 (Wako Pure Chemical) were used as the starting materials. They were dried prior to use at 120–160°C for 5–10 h, weighed, and thoroughly mixed together with an agate mortar and a pestle. The intimate mixture was initially heated at 650°C for 2 h to expel carbon dioxide gas, and then calcined at 800°C for 12 h in a gold boat. The product was reground and uniaxially cold-pressed into a pellet (12 mm in diameter and 1.5–2 mm thick) at 250 MPa. The pellet was sintered at 1350°C for 1 h on a platinum boat in a covered MgO crucible and allowed to cool to room temperature in the furnace which was turned off. Typically, pellets had a porosity of 3–30%, which generally decreased with an increasing value of x.

A conductivity measurement cell was made by sputtering gold onto the opposite, flat faces of the sintered pellet after polishing with successive grades of lapping films. The cell was mounted between two outer gold electrodes of a conductivity jig, which was put in a Pyrex tube. The tube was immersed in a thermostatted oil-bath with a programmable temperature proportional integral differential (PID)-controller, whereby the temperature of the cell was controlled within ± 0.15°C in a range of -30 to 200°C. The cell was kept for more than 30 min at each temperature to achieve the temperature equilibrium prior to measurements. The a.c. impedance of the cell was measured with an impedance analyser (YHP 4192A) under an argon atmosphere over the frequency range, $f = 5$ Hz–13 MHz. The collected data were analysed in three interrelated formalisms [18], the complex impedance (Z^*), the complex admittance (Y^*), the complex modulus (M^*) to estimate bulk and total conductivity.

Powder X-ray diffraction analysis (XRD) was made with a Rigaku RAD-C system (Ni-filtered Cu Kα) and the Cell-series programs [19]. The diffraction data were usually collected at a scanning speed of 2° min^{-1} in an angular range of $5° < 2\theta < 100°$. For accurate measurements of the d-spacings, highly pure Si powder was added as an internal standard and the data were collected with a 2θ-step size of 0.05°.

Since Li volatilized inevitably during sintering, the Li content of the sintered pellet was determined by flame emission analysis (FEA). A small amount of the sample was dissolved with a hot, concentrated solution of ammonium hydrogensulfate, NH_4HSO_4, and diluted with distilled water. A standard addition calibration method was used.

3. Results and discussion

Fig. 1 shows the variation of XRD patterns versus x in the composition $Li_{2x}Sr_{1-2x}Fe_{0.5-x}Ta_{0.5+x}O_3$, indicating that a perovskite solid solution with a similar pattern formed in the range $x \leq 0.25$ by the substitution

$$2Sr^{2+} + Fe^{3+} \rightarrow 2Li^{+} + Ta^{5+}$$

The samples became mixtures of the solid solution and $LiTaO_3$ beyond the solid-solution limit. The variation for the Cr-containing compositions with x were quite similar to those of Fig. 1. Powder XRD data for the compositions $Li_{0.5}Sr_{0.5}M^{III}_{0.25}Ta_{0.75}O_3$ ($x = 0.25$, M = Fe, Cr) are given in Table 1. All the reflections were indexed in a simple cubic perovskite unit cell (space group: $Pm3m$; $a = 396.39$ pm for

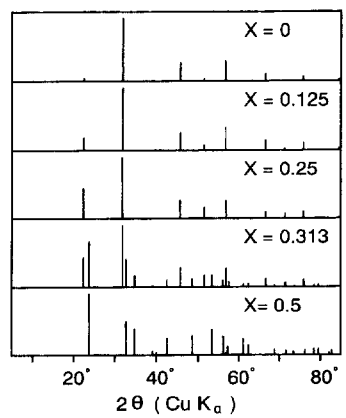

Fig. 1 Powder XRD patterns in the compositions $Li_{2x}Sr_{1-2x}Fe_{0.5-x}Ta_{0.5+x}O_3$.

Table 1
Powder XRD data for $Li_{0.5}Sr_{0.5}M^{III}_{0.25}Ta_{0.75}O_3$ ($x = 0.25$, M = Fe, Cr)

	M = Fe (*Pm3m*, cubic, $a = 396.39$ pm)			M = Cr (*Pm3m*, cubic, $a = 395.03$ pm)		
h k l	d_{obs} (pm)	d_{calc} (pm)	I_{obs}	d_{obs} (pm)	d_{calc} (pm)	I_{obs}
1 0 0	397.9	396.4	50	396.6	395.0	50
1 1 0	280.9	280.3	100	279.9	279.3	100
1 1 1	228.7	228.9	2	228.3	228.1	2
2 0 0	198.4	198.2	31	197.7	197.5	38
2 1 0	177.4	177.3	19	176.7	176.7	16
2 1 1	161.9	161.8	30	161.3	161.3	30
2 2 0	140.2	140.1	12	139.7	139.7	14
2 2 1 3 0 0	132.0	132.1	9	131.7	131.7	8
3 1 0	125.4	125.4	12	124.9	124.9	12
3 1 1		119.5		119.1	119.1	2
2 2 2	114.4	114.4	3	114.0	114.0	1

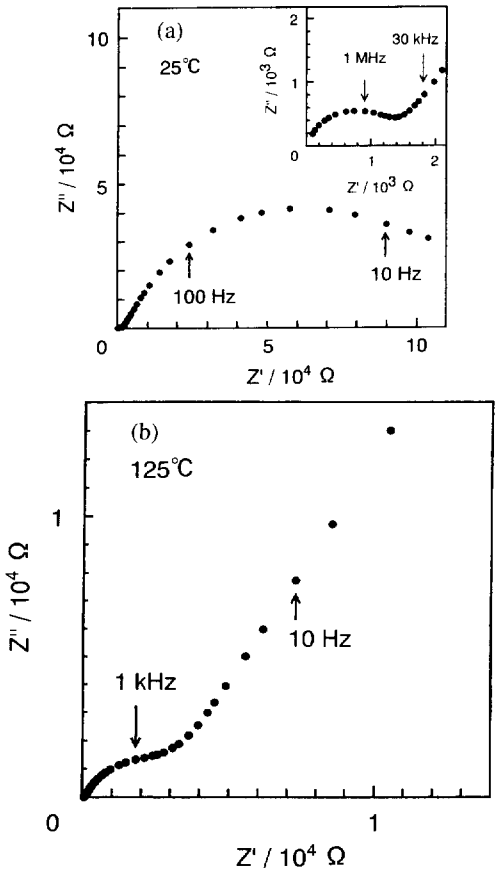

Fig. 2. Complex impedance plots of the composition $Li_{0.5}Sr_{0.5}Fe_{0.25}Ta_{0.75}O_3$ ($x = 0.25$). (a) at 25°C, and (b) at 125°C.

Fe, $a = 395.03$ pm for Cr); extra lines due to superstructure were absent. This indicates that the Li and Sr ions, and the M (Fe or Cr) and Ta ions are randomly distributed over the A- and B-sites, respectively. The lattice parameter, a, was constant in the whole range of solid solution formation in both systems (strictly speaking, an increase of about 1 pm from $x = 0.25$ to $x = 0$ for M = Fe). Polymorphic forms with different superstructural cells have been found for the $Li_{3x}La_{0.67-x}TiO_3$ solid solution [6,11,12]. We have obtained no evidence of the formation of ordered, perovskite-related phases with superstructure under preparation conditions tested to date. Annealing the sintered samples ($x = 0.25$) at 800°C resulted in precipitation of an unknown phase for the Fe-containing solid solution and $LiTaO_3$ for the Cr-containing solid solution, respectively.

The complex impedance plots of the sintered pellets with blocking gold electrodes, generated a typical response of ionic conductors with high conductivity [18,20,21]. Fig. 2(a) and (b) shows the complex impedance plots of the composition $Li_{0.5}Sr_{0.5}Fe_{0.25}Ta_{0.75}O_3$ ($x = 0.25$) at 25 and 125°C as typical examples. The plots at 25°C give a small semicircle in the high-frequency region (the above right figure inserted in Fig. 2(a)) and a large semicircle in the low-frequency region. The calculated parallel capacitance, C_p, associated with the high-frequency semicircle was ~57 pF, being one order of magnitude larger than those for bulk response of the usual cation-conducting oxides. This is not unusual because of high permittivity characteristics of perovskites. On the other hand, the C_p value associated with the low-frequency semicircle was ~40–50 nF, which is typical of a surface-layer effect [22] or a grain-boundary effect. The plot at 125°C gives a part of the low-frequency semicircle and an inclined spike due to double-layer capacitance, C_{dl}, at the blocking electrode–electrolyte interface. The C_p and C_{dl} values were ~40 nF and 2 μF, respectively. Their magnitudes were reasonable in view of their origins [18]. The spike is an indication that the sample is a nearly pure ionic conductor. Preliminary d.c. polarization measurements with a gold blocking electrode showed that their electronic transference numbers were at most 0.001 for both compositions (M = Fe, Cr; $x = 0.25$).

The explanation described above was confirmed by impedance and modulus spectroscopic plots (the imaginary parts of complex impedance and modulus, Z'', M'' versus log f). Fig. 3 shows the Z''–log f and M''–log f plots of the impedance data used in Fig. 2(a). The electrical modulus plots of the

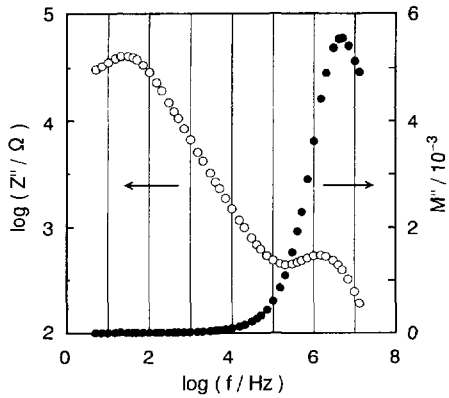

Fig. 3. Impedance and modulus spectroscopic plots (Z'' vs. log f, M'' vs. log f) for the data used in Fig. 2(a)

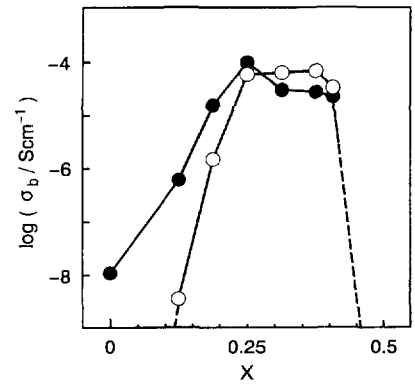

Fig. 4 Composition dependence of bulk conductivity in the compositions $Li_{2x}Sr_{1-2x}M^{III}_{0.5-x}Ta_{0.5+x}O_3$ (●) M = Fe, and (○) Cr

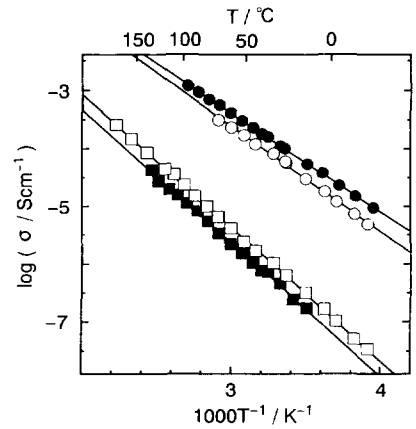

Fig. 5 Temperature dependence of (○) bulk conductivity and (□) total conductivity for the compositions $Li_{0.5}Sr_{0.5}M^{III}_{0.25}Ta_{0.75}O_3$ ($x = 0.25$) (closed symbols) M = Fe, and (open symbols) M = Cr.

equivalent circuit of polycrystalline electrolyte will give a Debye peak corresponding to every parallel R_pC_p element; however, a notable feature of the modulus plots is that the peak height of M'' is proportional to $1/C_p$ [18]. The R_pC_p elements corresponding to grain boundary response and electrode–electrolyte interfacial response will give extremely small and generally nondetectable peaks because their C_p values are relatively much too large. As we expected, only a large M'' peak due to bulk response is observed in the modulus plots shown in Fig. 3. The M'' peak shifted to a lower frequency with decreasing temperature, but no other peaks were observed, implying that the conductivity is isotropic [23]. The small, high-frequency Z'' peak and the M'' peak appear in roughly the same frequency range, demonstrating that the high-frequency semicircle can be assigned to bulk response again. A small difference in peak frequency is a common phenomenon, associated with dispersions in bulk a.c. conductivity and permittivity of a non-ideal, dispersive conductor [24].

Fig. 4 shows bulk conductivities at room temperature in both series. A maximum conductivity of 1.0×10^{-4} S cm^{-1} at 25°C was found at $x = 0.25$ near the high x limit of solid-solution formation for Fe, whereas a maximum conductivity of 7.0×10^{-5} S cm^{-1} (25°C), at $x = 0.375$ outside the formation range for M = Cr, in spite of the incorporation of a poorly conductive $LiTaO_3$. Sinterability was poorer for M = Cr than for M = Fe and increased with increasing Li content. The conductivity at $x = 0.25$ for M = Cr was 6.0×10^{-5} Scm^{-1} at 25°C, being slightly lower than the maximum value because of its higher porosity at $x = 0.25$. The conductivity for a denser sintered body is probably higher than the maximum value at $x = 0.375$. The maximum value for M = Fe is the highest of those reported to date for tantalate-based lithium electrolytes. The bulk conductivities abruptly dropped beyond $x = 0.375$; this is probably associated with a kind of percolation phenomenon of the mixed state between the conductive solid solution and non-conductive $LiTaO_3$.

Fig. 5 shows the temperature dependence of bulk and total conductivity for both solid solutions ($x = 0.25$). The data are plotted for the heating cycle only but the plots for the cooling cycle lie on the same lines. This implies that both perovskite phases are stable without phase transition in the temperature ranges. The total conductivities were lower than the bulk conductivities by a factor of 1/50–1/100. Such high additional resistance is common to the La-containing perovskites [5,6] and Li-substituted NASICONs [13,14], but not to γ-Li_3PO_4 solid solutions [25,26], which can be sintered at lower temperatures. The cause is probably associated with formation of a second phase in grain boundary region, which formation results from Li loss during high temperature sintering. The activation energies for Li-ion conduction, E_{Li}, and pre-exponential factors, σ_0, were calculated from the Arrhenius equation: $\sigma T = \sigma_0 \exp(-E_{Li}/kT)$, where σ is the conductivity, k the Boltzmann constant, and T the absolute temperature. The conductivity data are listed in Table 2. Their conductivity remained unchanged on prolonged standing for at least three months; they are more likely thermodynamically stable at room temperature. The Fe- and Cr-containing solid solutions are the first of tantalate-based perovskites with high Li-ion conductivity.

FEA on both solid solutions indicated that an Li loss of about 10% took place during sintering. We suggests that the Li loss occurs according to the following change

Table 2
Conductivity data for $Li_{0.5}Sr_{0.5}M^{III}_{0.25}Ta_{0.75}O_3$ ($x=0.25$, M = Fe, Cr)

M^{III}	Bulk			Total		
	σ, 25°C (S cm^{-1})	σ_0 (S cm^{-1} K)	E_{Li} (eV)	σ, 25°C (S cm^{-1})	σ_0 (S cm^{-1} K)	E_{Li} (eV)
Cr	6.0×10^{-5}	6.3×10^{4}	0.39	6.4×10^{-7}	3.1×10^{4}	0.49
Fe	1.0×10^{-4}	4.2×10^{4}	0.36	3.7×10^{-7}	1.7×10^{4}	0.49

σ: ionic conductivity at 25°C; σ_0: pre-exponential factor, E_{Li}: activation energy for Li ion conduction.

Table 3
Composition ranges of perovskite solid solutions in the compositions $Li_{2x}Sr_{1-2x}M^{III}_{0.5-x}Ta_{0.5+x}O_3$ (M = Co, Al, Ga, In, Y) and their conductivities

M^{III}	x range of solid solution formation	Conductivity at 25°C (S cm^{-1})
Co	<0.16	3×10^{-8} ($x=0.156$)
Al	no range	2.0×10^{-6} ($x=0.313$) [a]
Ga	<0.22	1.9×10^{-7} ($x=0.218$)
In	<0.16	4×10^{-8} ($x=0.156$)
Y	no range	4×10^{-8} ($x=0.125$) [a]

[a] Sample containing an unknown phase

$$\text{original composition} \rightarrow \underset{\text{(in grain)}}{\text{A-site deficient perovskite}} + \underset{\text{(in grain boundary)}}{\text{second phase}} + Li_2O\uparrow$$

This implies the formation of a corresponding amount of the A-site vacancies required for Li-ion conduction [6–8]. We have to optimize the ratio of Li-ion concentration to the A-site vacancy concentration for further improvement of the conductivity.

Table 3 summarizes the composition ranges of solid-solution formation in the other series and the conductivities of the perovskite solid solutions near to the high x-limits. For M = Co, Ga, In, solid solutions based on simple cubic perovskite formed in more limited ranges than those of M = Fe, Cr. In contrast to the solid solutions for M = Fe, Cr, the other solid solutions exhibited conductivities as low as 10^{-7}–10^{-8} S cm^{-1} at room temperature. For M = Al, Y, no samples of a single perovskite phase were obtained, but perovskite-related phases were observed as a major phase. However, high ionic conductivity was not found in these systems.

4. Conclusions

Formation of solid solutions with perovskite structure and ionic conductivity have been investigated in the series $Li_{2x}Sr_{1-2x}M^{(III)}_{0.5-x}Ta_{0.5+x}O_3$ (M = Cr, Fe, Co, Al, Ga, In, Y). Our conclusions are:

1. The compositions $Li_{0.5}Sr_{0.5}M^{III}_{0.25}Ta_{0.75}O_3$ (M = Fe, Cr; $x=0.25$) had high bulk conductivities of 1.0×10^{-4} and 6.0×10^{-5} S cm^{-1} at room temperature, respectively. The former value is the highest of those reported to date for tantalate-based lithium electrolytes.
2. They were simple cubic perovskites (space group: *Pm3m*; $a=396.39$ pm for Fe, $a=395.03$ pm for Cr), indicating that the Li and Sr ions, and the M (Fe or Cr) and Ta ions are randomly distributed over the A-sites and B-sites, respectively. The perovskite solid solutions formed in a relatively extensive range of $x \leq 0.25$ in both systems. The Fe- and Cr-containing solid solutions are the first of tantalate-based perovskites with high Li-ion conductivity.
3. Frame emission analysis for Li in the both sintered pellets revealed that the loss of Li took place during sintering. The high conductivity is probably attribute to an A-site deficient perovskite phase resulting from the loss.
4. Solid solutions based on a simple cubic perovskite formed in ranges of $x \leq 0.22$ for M = Ga, and $x < \sim 0.16$ for M = Co, In. The perovskite solid solutions in these systems exhibited conductivities as low as 10^{-7}–10^{-8} S cm^{-1} at room temperature.

Acknowledgements

J.K. thanks SUT for a research grant. Thanks are also due to the late Professor Y. Takaki for offering the Cell-series programs of XRD analysis, Y. Harada for his experimental assistance, and Y. Yamada (Yamakitsu System Ware, Nagoya) for building the software for a.c. impedance measurement.

References

[1] T. Takahashi (ed.), *High Conductivity Solid Ionic Conductors*, World Scientific, Singapore, 1989.
[2] G Pistoia (ed.), *Lithium Batteries*, Elsevier, Amsterdam, 1994, Ch. 10, pp 377–416.
[3] C.F. Holmes, in G. Pistoia (ed.), *Lithium Batteries*, Elsevier, Amsterdam, 1994, Ch. 10, pp 377–416.
[4] A.G Belous, G.N. Novitskaya, S.V. Polyanetskaya and Yu.I. Gornikov, *Izv. Akad. Nauk SSSR., Neorg. Mater., 23* (1987) 470–472
[5] Y. Inaguma, C. Liquan, M. Itoh and T Nakamura, T. Uchida, H. Ikuta and M Wakihara, *Solid State Commun., 86* (1993) 689–693.
[6] H. Kawai and J Kuwano, *J Electrochem. Soc., 141* (1994) L78–L79
[7] H Kawai and J. Kuwano, in P. Vincenzini (ed.), *Advances in Science and Technology 3D, Ceramics. Charting the Future, Proc. 8th CIMTEC World Ceramic Congress, Florence, Italy, June 1994*, TECHNA srl, Faenza, 1995, pp. 2641–2648
[8] Y. Inaguma, C. Liquan, M. Itoh and T. Nakamura, *Solid State Ionics, 70/71* (1994) 196–202

[9] Y Inaguma, Y. Matsui, Y. Shan, M Itoh and T. Nakamura, *Solid State Ionics*, 79 (1995) 91–97
[10] J.M.S. Skakle, G.C. Mather, M. Morales, R.I. Smith and A.R. West. *J. Mater Chem.*, 5 (1995) 1807–1808.
[11] A.D. Robertson, S.G Martin, A. Coats and A R West. *J Mater. Chem*, 5 (1995) 1405–1412.
[12] A. Várez, F Gracía-Alvarado, E. Moán and M A Alario-Franco, *J Solid State Chem.*, *118* (1995) 78–83.
[13] M A Subramanian, R. Subramanian and A Clearfield, *Solid State Ionics*, *18/19* (1986) 62–569.
[14] H. Aono, E Sugimoto, Y Sadaoka, N. Imanaka and G Adachi, *J Electrochem. Soc.*, *137* (1990) 1023–1027
[15] C Delmas, A. Nadiri and J.L. Soubeyoux, *Solid State Ionics*, *28–30* (1988) 419–423.
[16] Y Shan, Y. Inaguma and Y. Inaguma, *Preprints Annual Meet. Ceramic Soc Japan*. The Ceramic Society of Japan, Tokyo, 1995, p. 76.
[17] M Itoh, Y. Inaguma, W Jung, L. Chen and T. Nakamura, *Solid State Ionics*, *70/71* (1995) 203–207.
[18] I.M. Hodge, M D Ingram and A R. West, *J. Electroanal Chem.*, *74* (1976) 125–143.
[19] Y Takaki, T Taniguchi and H Hori, *J. Ceramic Soc. Jpn.*, *101* (1993) 373–376.
[20] R D. Armstrong, T. Sickinson and P.M. Wills, *J. Electroanal. Chem.*, *53* (1974) 389–405
[21] M.L. Bayard and G.G. Barna, *J. Electroanal Chem.*, *91* (1978) 201–209.
[22] C C. Hunter, M D Ingram and A.R. West, *J. Mater. Sci. Lett.*, *1* (1982) 522–524
[23] R J Grant, M D. Ingram and A.R West, *Electrochim Acta*, *22* (1977) 729–734.
[24] D.P. Almond and A R West, *Solid State Ionics*, *11* (1983) 57–64
[25] J Kuwano and A R West, *Mater Res Bull*, *15* (1980) 1661–1667
[26] A.R Rodger, J Kuwano and A R West, *Solid State Ionics*, *15* (1985) 185–198